International Journal of Mechanical, Industrial and Aerospace Sciences
ISSN: 2517-9950
Vol:4, No:12, 2010

An Investigation to Effective Parameters on the Damage of Dual Phase Steels by Acoustic Emission Using Energy Ratio

A. Fallahi, R. Khamedi

***Abstract*—**Dual phase steels (DPS)s have a microstructure consisting of a hard second phase called Martensite in the soft Ferrite matrix. In recent years, there has been interest in dual-phase steels, because the application of these materials has made significant usage; particularly in the automotive sector Composite microstructure of (DPS)s exhibit interesting characteristic mechanical properties such as continuous yielding, low yield stress to tensile strength ratios(YS/UTS), and relatively high formability; which offer advantages compared with conventional high strength low alloy steels(HSLAS). The research dealt with the characterization of damage in (DPS)s. In this study by review the mechanisms of failure due to volume fraction of martensite second phase; a new method is introduced to identifying the mechanisms of failure in the various phases of these types of steels. In this method the acoustic emission (AE) technique was used to detect damage progression. These failure mechanisms consist of Ferrite-Martensite interface decohesion and/or martensite phase fracture. For this aim, dual phase steels with different volume fraction of martensite second phase has provided by various heat treatment methods on a low carbon steel (0.1% C), and then AE monitoring is used during tensile test of these DPSs. From AE measurements and an energy ratio curve elaborated from the value of AE energy (it was obtained as the ratio between the strain energy to the acoustic energy), that allows detecting important events, corresponding to the sudden drops. These AE signals events associated with various failure mechanisms are classified for ferrite and (DPS)s with various amount of Vm and different martensite morphology. It is found that AE energy increase with increasing Vm. This increasing of AE energy is because of more contribution of martensite fracture in the failure of samples with higher Vm. Final results show a good relationship between the AE signals and the mechanisms of failure.

***Keywords*—**Dual phase steel (DPS)s, Failure mechanisms, Acoustic Emission, Fracture strain energy to the acoustic energy.

I. Introduction

THE typical microstructure of Dual phase steel (DPS) consist of a strong second phase of martensite within a soft ferrite matrix. These steels are one of the branches of high strength low alloy steels (HSLAS) which has highly desirable mechanical properties like continuous yielding, higher initial work hardening rate, uniform and total elongation, ductility, toughness, ultimate tensile strength, cold formability, and lower YS/UTS ratio. This combination of high tensile strength and good ductility is obviously a major advantage in DPSs compared with other high strength steels [1]-[5].

Acoustic Emission (AE) is stress wave produced by sudden movement in stressed materials. Sudden movement at the source produces a stress wave, which radiates out into the structure and excites a sensitive piezoelectric transducer [6].

Thorough investigation of AE during the deformation of all types of metals and composites can improve the understanding of the dynamic processes of deformation and fracture. Given the complexity of DPSs, and the dynamic processes of deformation and fracture, studying the microstructural effects on deformation and fracture is of compelling interest.

Some researchers report that the type of damage sustained in DPSs involves only ferrite/martensite decohesion [7]-[8], however, other research shows that this damage can also entail martensite fracture [3]-[4] and [9]-[11]. In order to recognize the types of damage sustained fractography [12]-[13] and in situ tests [14] were applied.

With respect to the above review, it is apparent that there is no overriding consensus about the mechanisms of damage in DPSs.

This paper studies the effect of various volume fractions of martensite (Vm)s and morphologies of martensite on the behavior of AE under tensile loading. To achieve this aim, a new function (that defined by fracture energy to the acoustic energy), was applied to provide relevant information from AE signals to distinguish various types of damage. The results reveal a strong relationship between failure modes and AE based analysis.

II. Experiments Procedure

The DPS in this study is produced from low carbon steel the composition of which is shown in table I. Also the composition of pure ferrite and martensite which heat treated is shown in table I. The 12 mm thick hot rolled sheet with a low impurity of Sulphurous and Phosphorus was chosen to minimize the effects of coarse inclusions. Standard samples for tensile testing were produced by machining 6.9 mm width, 2.4 mm thickness and 35 mm gauge length dimensions. These samples were heated for 20 min at 920 $^{\circ}C$ and then air-cooled. For this study, the A_1 and A_3 temperatures were calculated to be 709 $^{\circ}C$ and 848 $^{\circ}C$, respectively as mentioned by Leslie [15].

A. Fallahi and R. Khamedi are with the Department of Mechanical Engineering, Amirkabir University of Technology, 424 Hafez Ave., Tehran 15916-34311, Iran. (e-mail: afallahi@aut.ac.ir; Khamedi@aut.ac.ir).

TABLE I
CHEMICAL COMPOSITIONS OF THE USED STEELS (WT.%)

DPS	C	Mn	Si	Al	Nb
	0.0936	1.2937	0.0127	0.03	0.0147
	P	S	Cu	Fe	
	0.0129	0.0058	----	Bal.	
Ferrite	C	Mn	Si	P	S
	0.003	0.310	0.030	0.025	0.040
	Cu	Fe			
	0.032	Bal.			
Martensite	C	P	S	Fe	
	0.43	0.0181	0.009	Bal.	

TABLE II
MORPHOLOGIES AND ROOM TEMPERATURE TENSILE PROPERTIES OF DPS AFTER HEAT TREATMENT

Heat treatment temperature °C (Samples codes)	Ferrite grain size (μm)	*YS*	*UTS*	ε^*_u (%)	ε^*_t (%)	n	Strain Interval (%)	Vm (%)
730(IA730)	11.7	347	597	16	21	0.165	0.46-1.8	12
						0.24	1.8-8.2	
						0.13	8.2-16	
760(IA760)	11	386	850	11.5	16.5	0.31	0.4-1.65	34
						0.25	1.65-4.2	
						0.11	4.2-11.5	
790(IA790)	8.9	472	1030	9	12	0.28	0.6-2	49
						0.18	2-9	
820(IA820)	6.2	526	1160	7	9.7	0.6	1.1-1.6	65
						0.31	1.6-3	
						0.12	3-6.8	
Ferrite(F)	9.6	286	587	25	29.5	0.26	1.4-25	-----
730(F730)	10.2	279	461	20	31.3	0.23	2.2-10.2	-----
						0.11	10.2-20	
820(F820)	11.2	268	544	24.6	29.8	0.25	1.4-24.6	-----
920(F920)	53.1	160	322	19.5	23	0.27	1-19.5	-----
920(C40 Martensite)	------	1550	2100	----	1	0.56	0.65-1	≈100

By heating to intercritical temperature $(\alpha+\gamma)$ between $712^{\circ}C$ and $830^{\circ}C$ and implementing iced brine quenching in $(-8)^{\circ}C$, dual-phase microstructure (Ferrite-Martensite) can produced. This treatment was done for some intercritical temperatures, such as 730, 760, 790 and $820^{\circ}C$. Also, for the sake of understanding the effect of each martensite and ferrite phases on the AE signals, samples of pure ferrite and fully martensite (produced by the heat treating of C40 steel) were produced. The influence of ferrite grain sizes effect on the AE signals was investigated by full annealing of the pure ferrite samples at $920^{\circ}C$, $820^{\circ}C$ and $730^{\circ}C$.

After the heat treatment, cross-sections of the samples were polished, etched with 2% nital, and observed under the optical microscope to reveal their microstructure. The quantitative measurements were conducted using Image-Pro plus image analysis software. Then, using 20 to 30 images taken from different locations in the sample, an average Vm was determined. To measure the ferrite grain size, the Jeffries' method was employed to measure the equivalent area diameter grain size for different samples [16]. Figure 1 shows the microstructures. Table 2 shows room temperature tensile properties of DPS after heat treatment.

Uniaxial tensile tests were conducted at room temperature under displacement control using an INSTRON 8032 testing machine with a 250 kN load-cell, and cross-head speed of 0.05 mm/sec. The AE analysis is performed using an AE detector (PCI-DSP4) made by Physical Acoustic Corporation (PAC) with a PAC Nano30 transducer with the peak frequency of 446.88 kHz, setting up the amplitude threshold at 30 dB. The data processing has been done under the condition of a pre-amplification of 40 dB. The sensor was coupled to the polished specimens using grease under constant pressure.

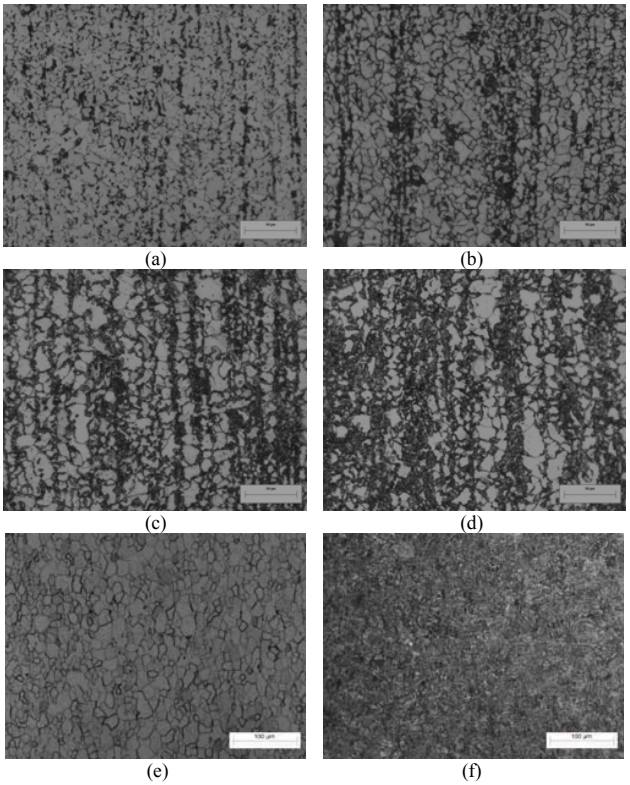

Fig. 1. The microstructures of a: IA730, b: IA760, c: IA790, d: IA820, e: F820 and f: C40 Martensite

III. FRACTURE ENERGY TO THE ACOUSTIC ENERGY RATIO

In order to better study of DPS internal behavior, a function is used, [17]-[19] identified as:

$$f(x) = Ln\left(\frac{E_s(x)}{E_{ac}(x)}\right) \quad (1)$$

Where E_S is strain energy, E_{ac} is cumulative acoustic energy and x is the driving variable (Displacement, Time or Strain). Depending on the internal behavior of material during the test, the $f(x)$ can pretend any combination of the four shape (increasing (P_I), sudden drop (P_{II}), constant (P_{III}) and decreasing (P_{IV}) shown in Fig. 2.

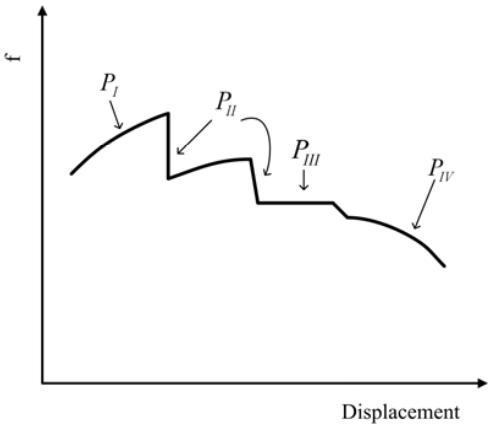

Fig. 2. Typical Sentry function

In fact, the increasing trend $P_I(x)$ is due to storing of strain energy, E_S, without prominent damage detection.

The sudden drops represented by $P_{II}(x)$, when an important internal material failure happens. The constant behaviors shown by $P_{III}(x)$ is due to a progressive strain energy storing phase that is superimposed to an equal material damage progression, and the decreasing function $P_{IV}(x)$, is because of greater AE activity than the strain energy storing capability of the material. This is a sign for initiation of failure.

IV. Results and Discussion

A. Tensile test

In accordance with the results of tensile test in table2 and in agreement with other researchers [1]-[4], the YS and UTS, increase, and ε_u and ε_t decrease by increasing Vm. One of the results about the amount of work hardening exponent is notable. In the first steps of plastic deformation for IA820, it seems the amount of *"n"* is higher than usual. Comparing with the amount of *"n"* for *"C40 Martensite"* samples, apparently martensite phase sustains the main part of load. Presumably it is because of the creation process of martensite in the *"IA"* samples. In the *"IA"* samples, increasing the temperature over *"A_1 line"* crystallization of austenite grains take place on the ferrite grain boundaries. After quenching, the austenite converts to the martensite, and the microstructure consist of a semi continuous martensite phase that involves ferrite islands. While the Vm increase, in this sample, because of its microstructure, work hardening exponent is close to that of martensite.

B. Acoustic emission

Figures 3 to 7 indicate that the change in Vm, results different behavior of AE.

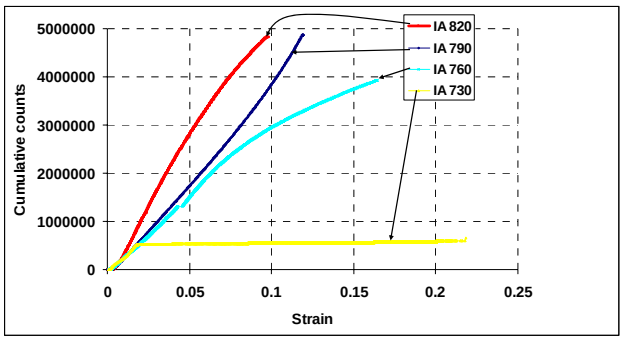

Fig. 3. Cumulative counts of all samples versus strain.

Considering the diagram of AE event cumulative counts, figure 3, it can be observed that in the IA730 sample, the low slope during yielding, then AE event cumulative counts of the diagram is almost constant. In the IA760 case, the slope of the diagram is almost constant up to near UTS and after that its slop decrease gradually. The important point is the high amount of AE cumulative counts comparing to the previous sample. This is because of higher Vm in this sample. In the cases with high Vm (IA790 & IA820), the cumulative counts exhibit an initial trend with low slope values in adjacency of yield, that increase after yield, they change to a semi constant slope to fracture. These AE cumulative counts are nearly like together and exhibit that up to $\sigma_{0.2}$, AE counts increase gradually comparing to after yield, but after yield, AE activities increase up to final fracture. This is because of internal behavior of these steels with high amount of Vm. Some failure behaviors like ferrite-martensite phases decohesion and martensite phase fracture is the basic elements that create this amount of AE cumulative counts.

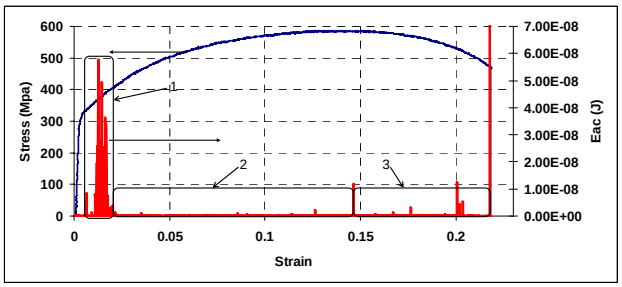

(a)

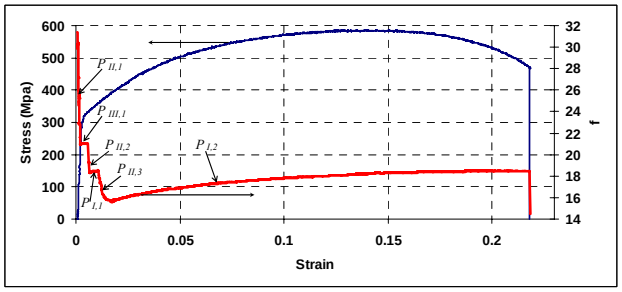

(b)

Fig. 4. IA730, (a) AE energy, (b) function f and stress versus strain.

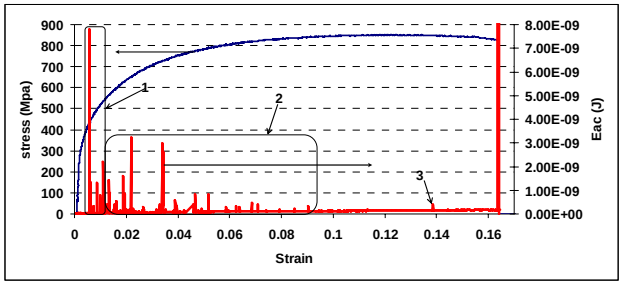

(a)

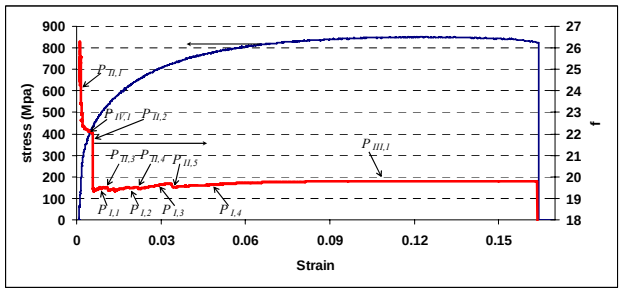

(b)

Fig. 5. IA760, (a) AE energy, (b) function f and stress versus strain.

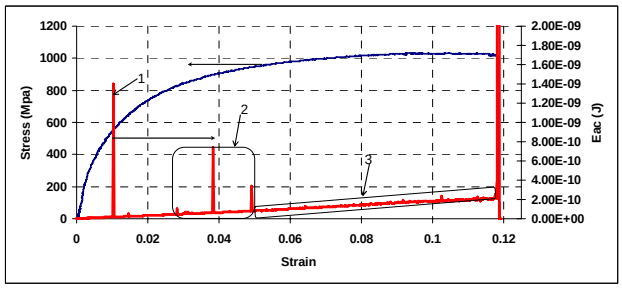

(a)

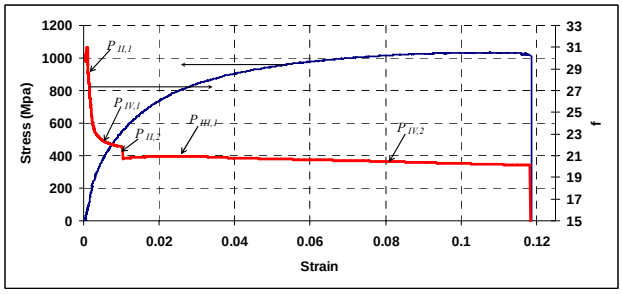

(b)

Fig. 6. IA790, (a) AE energy, (b) function f and stress versus strain.

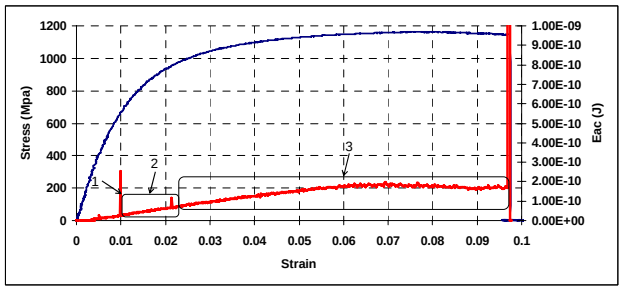

(a)

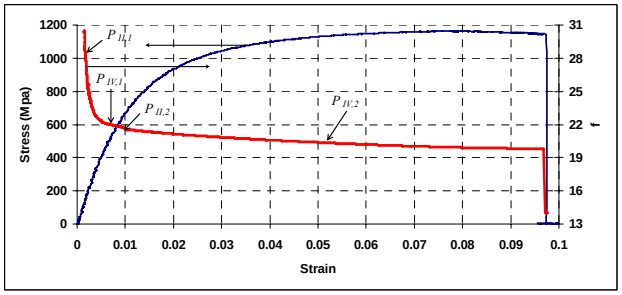

(b)

Fig. 7. IA820, (a) AE energy, (b) function f and stress versus strain.

Similar explanation of DPS behavior is also supported by the AE energy content. Figure 4a exhibits that around UTS, AE event energy increase. After UTS and before final fracture, at the nonuniform plastic deformation zone, AE event energy increases. The maximum AE energy of IA730 is about 5.75×10^{-8}J and it is surrounding $\sigma_{0.2}$. In the figure 5a, other than $\sigma_{0.2}$, this trend shifts to yield stress and between yield and UTS, and it is perhaps because of decohesion of ferrite and martensite in region 2. A weak AE energy is appearing during UTS and after UTS and it is possibly the result of martensite phase fracture [20]. Alike the previous samples, figures 6a and 7a show suddenly energy increase around $\sigma_{0.2}$ (region 1), this is because of material yield. Region 2 in these figures maybe shows the ferrite-martensite phases decohesion, and region 3 is because of martensite phase fracture [20]. The plastic deformation of materials generates acoustic emission that reaches the maximum at or near the yield point at the onset of macroplastic deformation resulting from the simultaneous motion of many dislocations [21]. Martensite phase creation is associated with expansion and a change of austenite phase volume leads to creation a large amount of mobile dislocations in the ferrite phase. Therefore, by increasing Vm, the amounts of mobile dislocations in ferrite phase increase. Near $\sigma_{0.2}$, these mobile dislocations move with high velocity and AE appears, after macroyielding starts, the AE decreases continuously because the dislocation velocity decreases [22]. This results show with the new function (*f*), internal behavior monitoring of DPS by AE is possible. Figure 4b exhibits that around the yield strength the "f" function has an almost decrease and this is because of high amount of AE activities in this part. After this part it increases with a low slope and this slope decreases gradually up to final fracture. This shows the lower AE released energy than fracture strain energy. This is probably because of gradual damage process in the sample with low Vm. In this sample failure is due to only ferrite-martensite phases decohesion [4], [20], [23], [24]. By increasing the strain, AE activities increase and this is the reason for decreasing *"f"* functions slope. By comparing the last part of *"f"* function (after $\sigma_{0.2}$) in these 4 samples, it is clear that for IA730, $P_{I,2}$ is ascendant, for IA760, $P_{III,1}$ is constant, for IA790, $P_{IV,2}$ is descent and for IA820. $P_{IV,2}$ is descent with higher slope. This means that with increasing Vm, the AE activities ratio to strain energy after yield, increase and the

reason for this phenomena is addition of second mechanism of failure (martensite phase fracture) to the first mechanism (ferrite-martensite phases decohesion). The contribution of martensite phase fracture is higher for the samples with high Vm [20], [23], [24].

The *"f"* function for the ferrite samples is almost similar together; especially for the samples which are heat treated. The main part of decreasing in the *"f"* function is for macro yielding and after this point, *"f"* changes to ascendant status (Fig. 8). Higher value of the *"f"* function for ferrite sample without annealing might be investigated.

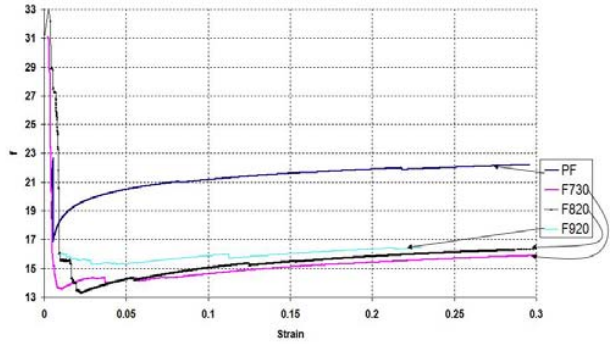

Fig. 8. *"f"* function versus strain for ferrite samples

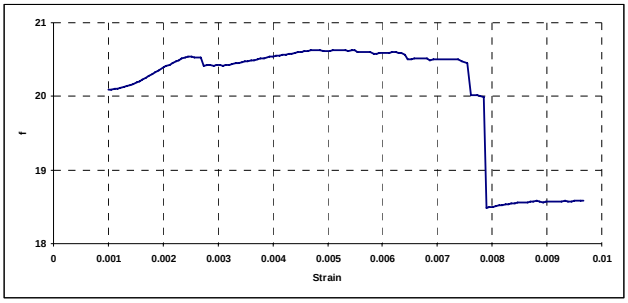

Fig. 9. *"f"* function versus strain for martensite sample

This function for martensite is shown in fig. 9 and exhibits a main part with constant amount of *"f"* (P_{III}) and a great drop (P_{II}) during fracture.

According to the Fig. 10, the amount of integral of *"f"* function $\left(\int f\, d\varepsilon\right)$ is equal to 3.87 for IA730, 3.27 for IA760, 2.46 for IA790, and 1.98 for IA820. This fact is because of decrease of fractrue strain and also the AE energy increase with increasing the Vm. In addition to these tests, some of the samples with fibrous martensite morphology have produced by intermediate quenching (IQ) process. In this heat treatment, the samples held at $920^{\circ}C$ ((γ) region) for 20 min, brine quenched in $-8^{\circ}C$, reheated to the mentioned intercritical temperatures, held for 20 min, and brine quenched in $-8^{\circ}C$. This heat treatment resulted fibrous martensite morphology. Comparing the AE sustained and analyzed, for IA and IQ samples, a notable difference due to the morphology of martensite is revealed. For example all of the *"f"* functions for the IQ samples are descending, and this point exhibits higher AE activities in these samples. Detailed discussion will report in the other paper.

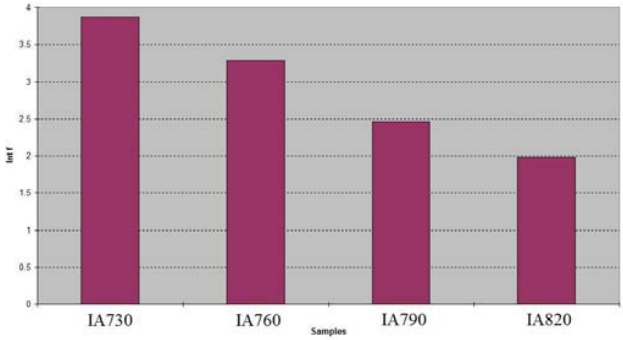

Fig. 10. Integral of "f" $\left(\int f\, d\varepsilon\right)$ for IA samples

Other than these analysis, according to [23]-[25], frequency spectrum analysis have done on the AE waveforms and the frequency range for ferrite deformation was between 150-175 kHz, for martensite was in the range of 520-700 kHz. Most of peak frequency of AE after yield for the IA730 and IA760 is in the range of 110-120 kHz. For the IA790 and IA820 samples, the peak frequency of AE after yield is in two ranges (102-131 kHz and 558-680 kHz). This is a support for the authors previous works and also a support for the discussions in this paper.

V. Conclusion

In this research, the AE behavior during the tensile testing of a range of DPSs with various Vms was examined and a new methodology was established for the post-processing of strain energy to AE energy ratio. The results show increasing AE energy with increasing the Vm. The integral of the *"f"* function $\left(\int f\, d\varepsilon\right)$ for the samples with high Vm is lower than the others. This fact is because of decrease of fracture strain and also the AE energy increase with increasing the Vm. In agreement with the previous works of the authors more contribution of martensite failure mechanism in the samples with high Vm leads to increasing of AE energy. The other analysis in this paper is based on frequency spectrum analysis. Frequency range for ferrite deformation is between 150-175 kHz and for martensite is in the range of 520-700 kHz. This range for ferrite-martensite decohesion is about 110-130 kHz.

Acknowledgment

The authors would like to thank Professor G. Minak and Dr. A. Zucchelli for their precious help in setting up the experimental tests at University of Bologna and their effective discussions. Also we acknowledge Dr. A. Morri and Dr. F. Lotti for their help to provide the test samples.

References

[1] A. Fallahi, "Microstructure properties correlation of dual phase steels produced rolling process", J. of Mater. Sci. and Tech., Vol. 18, no.5, pp. 451-454, 2002.

[2] Bag A, Ray K K, Dwarakadasa E S. Influence of martensite content and morphology on tensile and impact properties of high-martensite dual-phase steels. Metall. and Mater. Trans 1999; 30(A):1193-1202.
[3] A. Fallahi, "The Effect of Heat Treatment on Fatigue and Tensile Properties of Dual - Phase Steel", Amirkabir J. of Sci. & Tech., vol. 2, no. 6, pp. 141-148, 1987.
[4] A. Fallahi, "Processing of dual phase steels by controlled rolling" PhD Thesis, Sheffield University, 1990
[5] G. Thomas , J. H. Ahn, N. J. Kim, Controlled rolling process for dual phase steels and application to rod, wire, sheet and other shapes, United States Patent 4619714, 1986
[6] J. R. Davis (ed.), ASM Handbook: Volume 17, Nondestructive Evaluation and Quality Control, ASM International, Materials Park, OH, 1994.
[7] Korzekwa D A, Lawson R D, Matlock D K, Krauss G. A consideration of models describing the strength and ductility of dual-phase steels. Scripta Metallurgica 1980;14:1023-1028
[8] Speich G R, Miller R L. Mechanical properties of ferrite-martensite steels, structure and properties of dual-phase steels. Edited by Kot R A and Morris J W, TMS-AIME, New York: 1979, p. 145-182.
[9] Rashid M S, Cperk E R, Relationship between microstructure and formability in two high-strength low alloy steels. Formability Topics – Metallic materials, ASTM STP 647, American Society for Testing and Materials, Philadelphia, Pa, p. 174-190
[10] Balliger N K, Gladman T. Work hardening of dual-phase steels. Metal. Science 1981:15(3):95-108.
[11] Sun Sh, Pugh M. Properties of thermomechanically processed dual-phase steels containing fibrous martensite. Mater. Sci. and Eng. A 2002; 335:298–308.
[12] Jardim O R, Longo W P, Chawla K K. Fracture behaviour of a tempered dual phase steel. Metallography 1984; 17:123-130.
[13] Mediratta S R, Ramaswamy V, Rao P R. Influence of ferrite-martensite microstructural morphology on the low cycle fatigue of a dual-phase steel. Int. J. Fatigue 1985; 7(2):107-115.
[14] Kang J, Ososkov Y, Embury J D, Wilkinson D S. Digital image correlation studies for microscopic strain distribution and damage in dual phase. Scrip Mater 2007; 56:999-1002.
[15] Leslie. William. C., The Physical Metallurgy of Steels, McGraw-Hill, (1981), pp. 257.
[16] M. Mazinani and W.J. Poole, Effect of Martensite Plasticity on the Deformation Behavior of a Low-Carbon Dual-Phase Steel, Metallurgical and Materials Transactions A, Volume 38A, February 2007, 328-339.
[17] G. Minak, P. Morelli and A. Zucchelli, Fatigue residual strength of circular laminate graphite–epoxy composite plates damaged by transverse load. Composites Science and Technology, Volume 69, Issue 9, July 2009, Pages 1358-1363.
[18] G. Minak and A. Zucchelli, Damage evaluation and residual strength prediction of CFRP laminates by means of acoustic emission techniques, Composite Materials Research Progress, Nova Science Publishers (2008) 165-207.
[19] Cesari F, Dal Re V, Minak G, Zucchelli A, Damage and residual strength of laminated graphite-epoxy composite circular plates loaded at the centre, Composites Part A, 38 (2007), 1163-1173.
[20] R. Khamedi, A. Fallahi , A. Refahi Oskouei, Effect of martensite phase volume fraction on acoustic emission signals using wavelet packet analysis during tensile loading of dual phase steels, Mater & Design 2010; 31/6:2752-2759
[21] Heiple C R, Carpenter S H, Acoustic emission produced by deformation of metals and alloys – a review: part I, J Acous Emission 1987; 6:177-207.
[22] Long Q Y, Huazi Y. Acoustic emission during deformation of dual-phase steels, Metall Mater Trans A 1990; 21(1):373-379.
[23] Khamedi R, Fallahi A, Zoghi H. The influence of morphology and volume fraction of martensite on AE signals during tensile loading of dual-phase steels. Int J Recent Trend Eng 2009;1(5):30–4.
[24] Khamedi R, Fallahi A, Refahi Oskouei A, Ahmadi M. The effect of martensite phase volume fraction of dual-phase steels on acoustic emission signals under tensile loading. NSU XVII, BHU, Varanasi; 2008.
[25] C.S. Lee, J.H. Huh, D.M. Li, and D.H. Shin, Acoustic Emission Behavior during Tensile Tests of Low Carbon Steel Welds, ISIJ Int. vol. 39, no. 4, pp.365-370, 1999.

A. Fallahi received the B.Sc. degree in metallurgical engineering from Sharif University of technology, Tehran, Iran in 1976, the M.Sc. degree in metallurgical engineering from UMIST, Manchester, UK, in 1986 and the Ph.D. degree in metallurgical and manufacturing process from Sheffield University, UK, in 1990. In 1984, he joined the faculty of mechanical engineering department at Amirkabir university of Technology, Tehran. Iran. The author's major field of study is research on DPS. He has authored or coauthored over 40 scientific and technological papers.

R. Khamedi received the B.Sc. degree in mechanical engineering from Amirkabir university of Technology, Tehran, Iran in 2003, the M.Sc. degree in mechanical engineering from TMU, Tehran, Iran in 2005. He is currently working towards the Ph.D. degree at the department of mechanical engineering, Amirkabir university of Technology. His basic area of interest is DPS failure mechanisms and AE monitoring.